Neurobiology of Disease 126 (2019) 76–84

Contents lists available at ScienceDirect

Neurobiology of Disease

journal homepage: www.elsevier.com/locate/ynbdi

Review

Minocycline attenuates brain injury and iron overload after intracerebral hemorrhage in aged female rats

Shuhui Dai[a,b], Ya Hua[a], Richard F. Keep[a], Nemanja Novakovic[a], Zhou Fei[b], Guohua Xi[a,*]

[a] Department of Neurosurgery, University of Michigan, Ann Arbor, MI, USA
[b] Department of Neurosurgery, Xijing Hospital, Fourth Military Medical University, Xi'an, Shaanxi, China

ARTICLE INFO

Keywords:
Aging
Intracerebral hemorrhage
Iron
Minocycline
Magnetic resonance imaging
Ferritin
Heme oxygenase-1
Microglia

ABSTRACT

Brain iron overload is involved in brain injury after intracerebral hemorrhage (ICH). There is evidence that systemic administration of minocycline reduces brain iron level and improves neurological outcome in experimental models of hemorrhagic and ischemic stroke. However, there is evidence in cerebral ischemia that minocycline is not protective in aged female animals. Since most ICH research has used male models, this study was designed to provide an overall view of ICH-induced iron deposits at different time points (1 to 28 days) in aged (18-month old) female Fischer 344 rat ICH model and to investigate the neuroprotective effects of minocycline in those rats. According to our previous studies, we used the following dosing regimen (20 mg/kg, i.p. at 2 and 12 h after ICH onset followed by 10 mg/kg, i.p., twice a day up to 7 days). T2-, T2*-weighted and T2* array MRI was performed at 1, 3, 7 and 28 days to measure brain iron content, ventricle volume, lesion volume and brain swelling. Immunohistochemistry was used to examine changes in iron handling proteins, neuronal loss and microglial activation. Behavioral testing was used to assess neurological deficits. In aged female rats, ICH induced long-term perihematomal iron overload with upregulated iron handling proteins, neuroinflammation, brain atrophy, neuronal loss and neurological deficits. Minocycline significantly reduced ICH-induced perihematomal iron overload and iron handling proteins. It further reduced brain swelling, neuroinflammation, neuronal loss, delayed brain atrophy and neurological deficits. These effects may be linked to the role of minocycline as an iron chelator as well as an inhibitor of neuroinflammation.

1. Introduction

Intracerebral hemorrhage (ICH) is a devastating stroke subtype with high mortality and morbidity rate. Lysis of red bold cells (RBCs) in the hematoma results in increased perihematomal iron content. Iron may trigger a cascade of deleterious events, which can lead to secondary brain injuries and irreversible neurological deficits years after ICH (Keep et al., 2012). The cytotoxicity of hemolysis-generated iron is related to oxidative stress and an inflammatory response (Xi et al., 2006). During the past decade, studies have found that preventing iron-mediated toxicity is a promising therapeutic strategy for ICH (Keep et al., 2012; Xi et al., 2006).

Sex and age are two major modifiers of brain injury after ICH. Studies have shown that ICH-induced brain damage is less in young female animals, which may be related to normal circulating estrogen (Xi et al., 2006). ICH-induced brain damage is also age dependent. ICH results in more severe brain injury and neurological deficits in aged animals than in young ones (Xi et al., 2006).

Minocycline, a broad-spectrum tetracycline, can protect against neurological impairment in animal models of traumatic brain injury, stroke and neurodegenerative disease *via* its anti-inflammatory properties including inhibiting microglia activation and matrix metalloproteinases (Murata et al., 2008; Wang and Dore, 2007). However, a study has also demonstrated that minocycline can chelate iron in cortical neuronal cultures (Chen-Roetling et al., 2009). Our previous studies have shown that systemic administration of minocycline attenuates brain injury and improves functional deficits after ICH by reducing iron overload in both young and aged male rats (Cao et al., 2018; Zhao et al., 2011). However, the effect of minocycline in female rats remains unknown. According to the initial Stroke Therapy Academic Industry Roundtable (STAIR) recommendations, further studies should be performed in females, aged animals and animals with comorbid conditions (Fisher et al., 2009). It should be noted that minocycline reduces ischemic brain infarcts in male rats but not female rats (Li and McCullough, 2009).

The current study used an ICH model in aged female rats to investigate changes in perihematomal iron content and iron handling proteins as well as brain injury at different time points after ICH. It next

* Corresponding author at: R5018 BSRB, University of Michigan, 109 Zina Pitcher Place, Ann Arbor, MI 48109-2200, USA.
E-mail address: guohuaxi@umich.edu (G. Xi).

https://doi.org/10.1016/j.nbd.2018.06.001
Received 12 March 2018; Received in revised form 29 May 2018; Accepted 3 June 2018
Available online 05 June 2018
0969-9961/

examined whether or not minocycline can reduce iron overload and attenuate brain injury after ICH in those aged female rats.

2. Materials and methods

2.1. Animals and establishment of ICH model

All experiments followed the animal procedure protocols approved by the University Committee on Use and Care of Animals, University of Michigan. Seventy-two 18-month old female Fischer 344 rats (National Institutes of Health, Bethesda, MD, USA) were used in the experiments. The rats had free access to food and water before and after surgery and were housed in a 12 h light/dark cycle. The study complies with the ARRIVE guidelines for reporting *in vivo* experiments. Randomization was carried out using odd/even numbers. The rats were anesthetized with pentobarbital (40 mg/kg, i.p.) while rectal temperature was maintained at 37.5 °C. Rats were positioned in a stereotactic frame; a midline incision was made and a burr hole 3.5 mm to the right of bregma was drilled. Autologous whole blood (100 μl) was withdrawn from the right femoral artery and injected into the right basal ganglia (coordinates: 0.2 mm anterior, 5.5 mm ventral, and 3.5 mm lateral to the bregma) (Nakamura et al., 2004) with a 26-gauge needle at a rate of 10 μl/min to induce ICH. At 5 min after infusion, the needle was removed slowly, the bone hole was sealed with bone wax and the skin incision was closed. As a control group, rats received an intracaudate injection of 100 μl saline instead of autologous arterial blood. All animals were injected with analgesic (carprofen, 5 mg/kg, s.c.) after surgery.

2.2. Experimental groups and drug administration

Seventy-two female aged rats received either ICH or saline. Six rats died from this study (mortality rate = 8%). Three rats died in the first part of study. One died in the saline control group during anesthesia. Two rats died in the ICH group (one for the day-7 study and the other for the day-28 study). Both died approximately 3 h after ICH induction. Three rats died in the second part. There was one rat in the ICH + Vehicle group and two rats in the ICH + Minocycline group. All three rats were for the day-28 study and were found dead 2–4 h after ICH. Those rats were already be randomized. In the first part of our study, ICH rats were euthanized at days 1, 3, 7 or 28 (n = 5–6 per time point). Saline controls were euthanized at days 7 or 28 (n = 5–6). Brains were used for histology. In the second part of the study, ICH rats were treated with vehicle (n = 17) or minocycline (20 mg/kg, i.p. at 2 and 12 h after ICH onset followed by 10 mg/kg, i.p., twice a day up to 7 days, n = 16). At days 7 or 28, rats (5–6 rats for the day 7 study and 10–11 for the day 28 study) were euthanized and brains were harvested for histology. All rats had MRI and behavioral tests at different time points.

2.3. Magnetic resonance imaging

T2-, T2*-weighted and T2* array MRI was performed at 1, 3, 7 and 28 days after ICH onset or saline injection as described previously(Cao et al., 2018). Experiments were carried out in a 9.4 Tesla horizontal bore scanner (Agilent Technologies, CA, USA), with two-channel quadrature radio frequency rat head coil (M2M Imaging Corporation, OH, USA). Rats were anesthetized with 1.5% isoflurane/air mixture and body temperature was maintained using a forced-air heating system. T2-weighted anatomical images were collected applying the following parameters: field of view (FOV) = 35 × 35 mm; slice thickness = 0.5 mm; matrix (RO × PE) = 256 × 128; repetition time (TR) = 4000 ms; effective echo time (TE_{eff}) = 60 ms. T2*-weighted images were collected using the following parameters: FOV = 35 × 35 mm; slice thickness = 0.5 mm; matrix (RO × PE) = 256 × 128; TR = 250 ms; echo time (TE) = 5 ms; flip angle (FA) = 20°. T2* array scanning was performed with an arranged TE (6, 11, 16, 21, 26, 31, 36, 41 ms) applying the following parameters: FOV = 35 × 35 mm; slice thickness = 1 mm; matrix (RO × PE) = 128 × 128; TR = 250 ms; FA = 20°.

Brain swelling was calculated by measuring ipsi- and contralateral hemisphere volumes based on seven every other T2-weighted images, centered on the anterior commissure layer (Ni et al., 2015). Swelling was calculated as: (ipsilateral − contralateral) / contralateral × 100%.

Brain tissue loss was estimated by ipsilateral ventricle enlargement at day 28. Ipsi- and contralateral ventricular volumes were measured on T2-weighted images by combining 5 ventricle areas multiplying the thickness (0.5 mm). Ipsilateral ventricular enlargement was calculated as: (ipsilateral − contralateral) / contralateral × 100%.

T2* lesion volumes (reflecting hematoma size at day 1 and brain iron deposition at day 28) were measured by combining the total areas and multiplying by the thickness (0.5 mm). All measurements were repeated three times using an image analysis system (ImageJ).

T2* array images were reconstructed at different echo times as R2* (1/T2*) mapping with Matlab software for further analysis. R2* values of three areas in the peri-hematomal region and their corresponding areas in the contralateral hemisphere were measured. R2* values were expressed as a percentage of (ipsilateral − contralateral) / contralateral × 100%. All measurements of MRI were carried out by a blinded investigator.

2.4. Immunohistochemistry

Brain immunohistochemistry was used to assess neuronal damage using loss of dopamine- and cAMP-regulated phosphoprotein, Mr 32 kDa (DARPP-32), staining. DARPP32 is abundant in striatal medium-sized spiny neurons. Immunohistochemistry was also used to assess upregulation in the iron handling proteins ferritin and heme oxygenase-1 (HO-1), and microglial activation using immunostaining for ionized calcium binding adapter molecule 1 (Iba-1). Immunohistochemistry was performed as described previously (Dang et al., 2017; Jin et al., 2013). Briefly, three consecutive coronal 18 μm thick sections from 1 mm posterior to the blood injection site with a 162 μm interval were collected and immunostained for DARPP-32 (1:250, Cell Signaling Technology), ferritin (1:250, Sigma), HO-1 (1:500, ENZO) or Iba-1 (1:250, Wako). Bilateral DARPP-32 positive areas were outlined and ipsilateral loss calculated as: (contralateral − ipsilateral) / contralateral DARPP-32 positive area. For ferritin, HO-1 and Iba-1 positive cell counting, five images (×40 magnification) were taken in the perihematomal area. All measurements were repeated three times with Image J by a blinded investigator.

2.5. Behavioral tests

Corner turn and forelimb use asymmetry tests were used to detect neurological deficits. The percentage of right turns was calculated in corner turn test, in which rats could turn either right or left to exit a 30° corner. Forelimb use asymmetry score was quantified as previously described (Hua et al., 2002). Both tests were carried out before ICH and at 1, 3, 7 and 28 days after ICH. The behavioral tests were performed by a blinded investigator.

2.6. Statistical analysis

All data were presented as mean ± standard deviation (SD) and analyzed using SPSS (v.24, SPSS Inc., Chicago, IL, USA). Mean values were compared between two groups by Student's t-test and 1-way or 2-way ANOVA was used for multiple-group comparisons with an additional Scheffe's multiple comparisons test when needed. Comparisons were considered as statistically significant when $p < 0.05$. The sample size was determined the same as our previous minocycline studies in aged male rats (Cao et al., 2018).

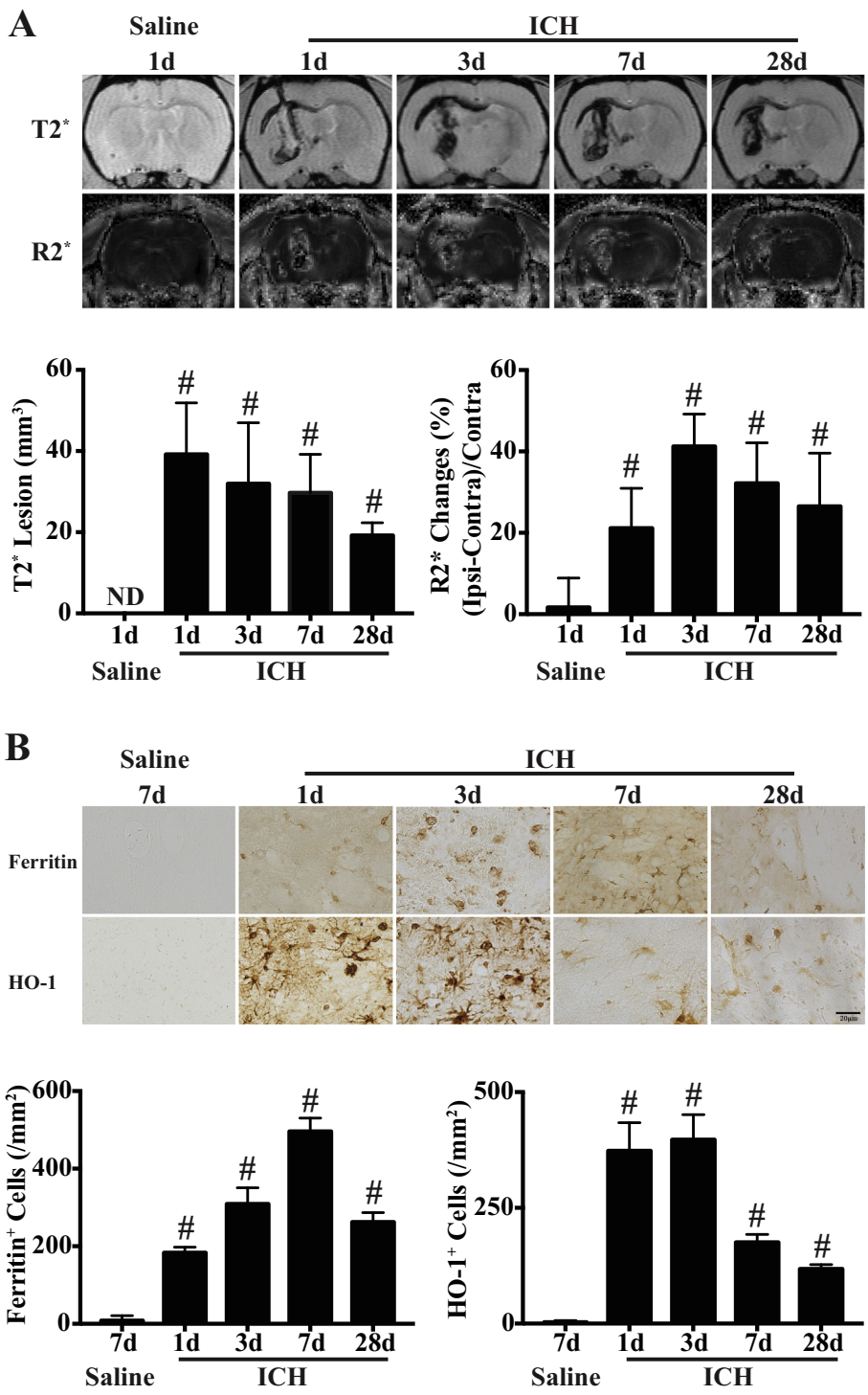

Fig. 1. ICH causes brain iron deposition and an increase in iron handling proteins in perihematomal areas in aged female rats. (A) Examples of T2*-weighted and R2* array MRIs taken 1 day after a saline injection or 1, 3,7 or 28 days after an ICH. Such imaging is quantified in the bar graphs. Values are means ± SD, $n = 5–22$, $^{\#}P < 0.01$ compared with saline group. ND = not detected. (B) Examples of ferritin and HO-1 immunohistochemistry in the ipsilateral basal ganglia at 7 days after a saline injection or 1, 3,7 or 28 days after an ICH (scale bar = 20 μm). The number of ferritin and HO-1 positive cells was quantified as shown in the bar graphs. Values are means ± SD, $n = 5$ in each group. $^{\#}P < 0.01$ compared with saline group.

3. Results

3.1. ICH induces iron overload in perihematomal area in aged female rats

ICH resulted in T2* lesions in the brain (reflecting hematoma at day 1 and brain iron overload at day 28). T2* lesions remained till 28 days although it decreased over time (Fig. 1A). Brain iron content was measured using T2* array scanning and shown as R2* (1/T2*) values. The operation and injection of saline did not cause variations in R2* values (Fig. 1A). Compared to the contralateral hemisphere, R2* values increased significantly at day 1 ($p < 0.01$, Fig. 1A) after ICH onset in perihematomal area. The R2* values were still significantly high at days 7 and 28 ($p < 0.01$).

Ferritin is an iron-storage protein regulated by cellular iron status (Truman-Rosentsvit et al., 2018). Compared with the saline controls, the number of ferritin positive cells increased significantly at day 1 ($p < 0.01$, Fig. 1B) post ICH and peaked at day 7 (496 ± 34 *vs* 8 ± 13 cells/mm^2 in saline group, $p < 0.01$, $n = 5$, Fig. 1B). HO-1 plays an important role in heme breakdown (Chen and Regan, 2007). In our study, the cells in the perihematomal areas expressing HO-1 increased rapidly at day 1 ($p < 0.01$, Fig. 1B) and peaked at day 3 post ICH (397 ± 54 *vs* 3 ± 4 cells/mm^2 in saline controls, $p < 0.01$,

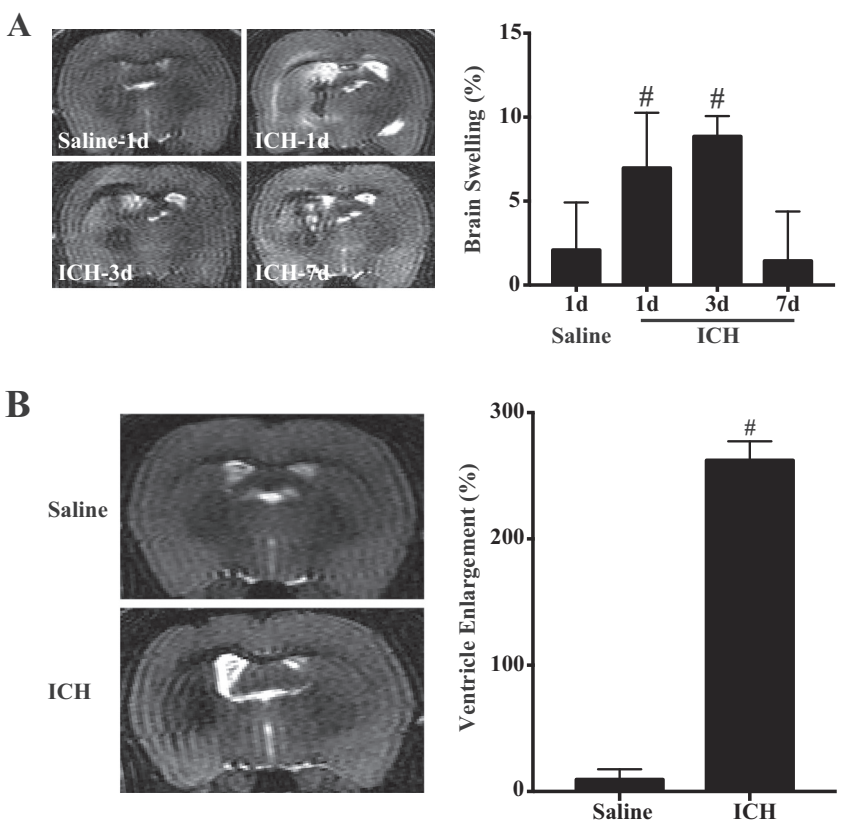

Fig. 2. ICH leads to acute brain swelling and chronic brain tissue loss in aged female rats. (A) Representative T2-weighted images over the first 7 days after ICH and a saline control (day 1). Such images were used to determine swelling in the ipsilateral hemisphere after ICH (n = 5–22) or a saline injection (n = 11). Values are means ± SD; $^{\#}P < 0.01$ compared with saline group. (B) Representative T2-weighted images at 28 days after ICH or a saline injection. Such images were used to determine ipsilateral ventricle enlargement in saline (n = 6) and ICH (n = 5) groups. Values are means ± SD; $^{\#}P < 0.01$ compared with saline group.

Fig. 1B).

3.2. ICH leads to brain damage, inflammation and neurological deficits in aged female rats

Brain swelling in the acute phase and brain tissue loss at day 28 were monitored by T2-weighted imaging after ICH (Mao et al., 2016). Compared with the saline group, brain swelling appeared at day 1 (6.98 ± 3.28 *vs* 2.09 ± 2.83%, $p < 0.01$, n = 11–22, Fig. 2A), reached a peak at day 3 (8.85 ± 1.21 *vs* 2.09 ± 2.83%, $p < 0.01$, n = 6–11, Fig. 2A) and decreased at day 7 (1.44 ± 2.94 *vs* 2.09 ± 2.83%, $p = 0.096$, n = 22–11, Fig. 2A) after ICH. Brain atrophy was assessed as ipsilateral ventricular enlargement compared to contralateral at day 28. That enlargement after ICH (262 ± 15%) was significantly greater than after saline injection (9.6 ± 8.1%, $p < 0.01$, n = 5–6, Fig. 2B).

DARPP-32 staining was used to assess neuronal loss in the basal ganglia in our study. There was a significantly greater decrease of DARPP-32 positive area at day 28 after ICH compared to saline controls (Fig. 3A). ICH also caused significant microglia/macrophage activation in the ipsilateral basal ganglia, which peaked at 3–7 days (Fig. 3B).

Forelimb use asymmetry scores and corner turn scores were used to measure behavioral deficits. Rats in the ICH group had a significant increase in the percentage of right (ipsiversive) turns compared with saline controls in the first week after ICH onset and a slow recovery took place with time. Similarly, the forelimb use asymmetry score increased significantly in the first week and decreased with time. By day 28 after ICH, there were still significant differences between ICH group and saline group in both corner turn scores and forelimb use asymmetry test scores (Fig. 3C).

3.3. Minocycline reduces ICH-induced iron deposition and iron handling protein upregulation in aged female rats

The effect of minocycline on brain iron overload in aged female rats was assessed at days 7 and 28 after induction of ICH. To make sure the results more reliable, we firstly measured the T2* lesion volume at day 1 of rats received vehicle and minocycline treatment separately. No significant diffidence was found in T2* lesion volume (Fig. 4A), indicating rats in the two groups had similar injury.

MRI showed systemic administration of minocycline significantly reduced T2* lesion volume at day 7 (21.5 ± 9.4 *vs* 30.3 ± 9.1 mm^3 in vehicle controls, n = 16–17, $p < 0.05$, Fig. 4A) and day 28 (9.4 ± 4.2 *vs* 18.3 ± 2.0 mm^3, n = 10–11, $p < 0.01$, Fig. 4A) after ICH. Similarly, R2* values significantly decreased in the minocycline-treated group compared to vehicle-treated group at day 7 ($p < 0.01$, Fig. 4A) and day 28 ($p < 0.01$, Fig. 4A).

Minocycline treatment significantly reduced the number of perihematomal ferritin positive cells at day 7 ($p < 0.01$, Fig. 4B) and day 28 ($p < 0.01$, Fig. 4B) compared with vehicle-treatment groups. HO-1 positive cells were also less in the minocycline-treated group than vehicle-treated animals at day 7 (55 ± 10 *vs* 175 ± 19 cells/mm^2, n = 5, $p < 0.01$, Fig. 4B) and day 28 (51 ± 9 *vs* 126 ± 22 cells/mm^2, n = 5, $p < 0.01$, Fig. 4B) after ICH onset.

3.4. Minocycline attenuates ICH-induced brain swelling and atrophy, inflammation, neuronal loss, and improves functional recovery in aged female rats

To investigate whether minocycline treatment influences ICH-induced brain injury in aged female rats, we analyzed brain swelling and ventricle volume on T2-weighted images. At day 3, brain swelling was decreased significantly in the minocycline-treated group compared to vehicle-treated rats (4.4 ± 2.9 *vs* 12.3 ± 4.5%, n = 6, $p < 0.01$, Fig. 5A). At day 28, there was a significant decrease of ventricle

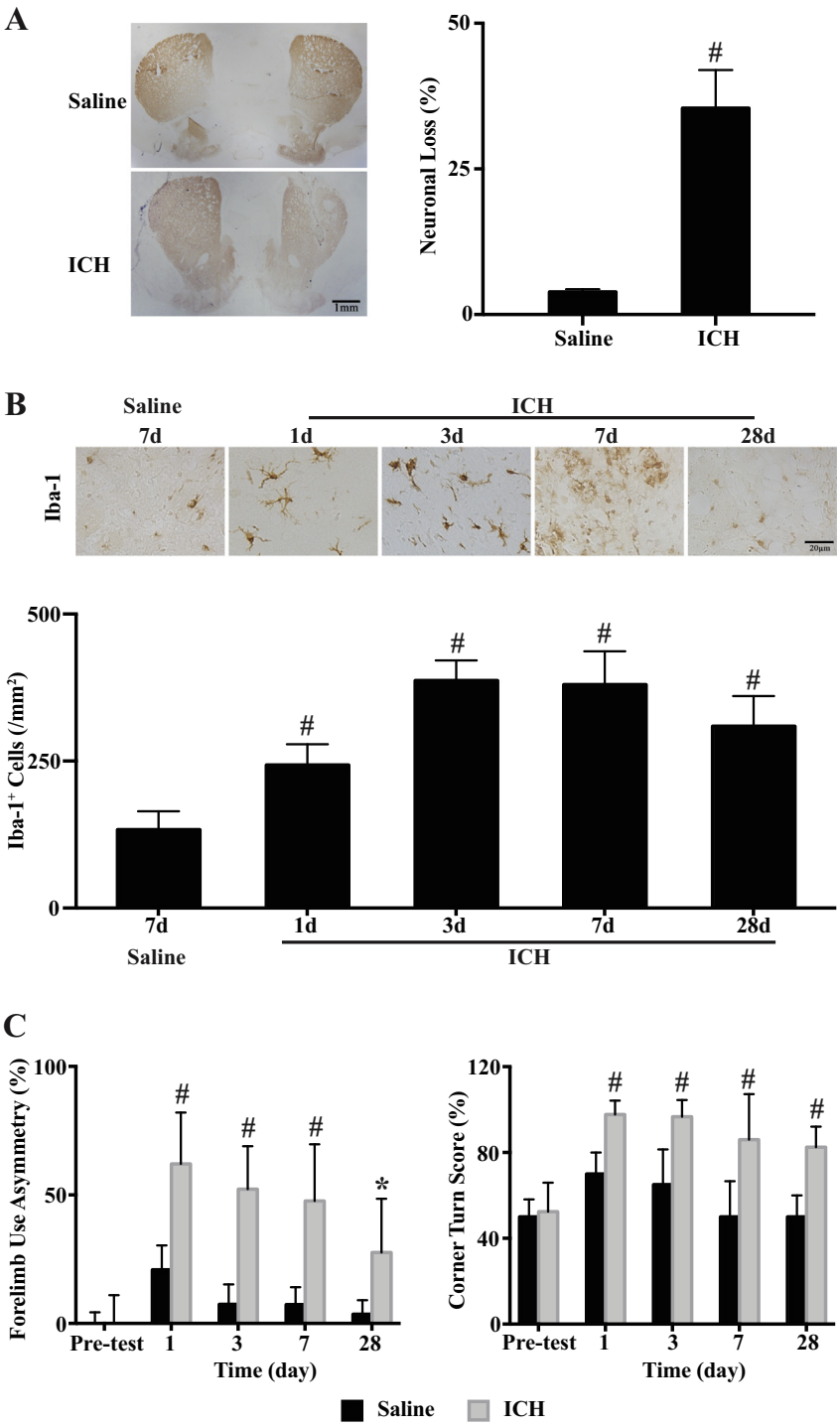

Fig. 3. ICH leads to neuronal loss, inflammation and neurological deficits in aged female rats. (A) Examples of DARPP-32 immunostaining at day 28 after a saline injection or an ICH. Note the ipsilateral shrinkage of the DARPP-32 positive area in the ICH rat. Scale bar = 1 mm. That loss was quantified in the bar graph. Values are means ± SD, $n = 5$ per group; $^{\#}P < 0.01$ compared with saline group. (B) Examples of micrographs showing microglia activation after ICH compared to saline control as assessed by the number of Iba-1 positive cells in the ipsilateral basal ganglia. Scale bar = 20 μm. The number of Iba-1 positive cells and presented in the bar graph. Values are means ± SD, $n = 5$ per group; $^{\#}P < 0.01$ *vs.* saline control. (C) Forelimb use asymmetry test and corner turn test were performed at different time points after ICH ($n = 5$–22) or saline control ($n = 6$–11). Values are means ± SD; $^{*}P < 0.05$ and $^{\#}P < 0.01$ compared with saline group.

enlargement in rats treated with minocycline compared with rats treated with vehicle (165 ± 54 *vs* 354 ± 69%, $n = 10$–11, $p < 0.01$, Fig. 5B), indicating that minocycline attenuated brain atrophy. Minocycline also attenuated ICH-induced microglia activation in the ipsilateral basal ganglia at days 7 and 28 (Fig. 5C).

Loss of DARPP-32 staining was used to quantify neuronal loss. While both minocycline and saline groups showed a reduction in the ipsilateral DARPP-32 positive area compared to contralateral at day 28 after ICH, that reduction was smaller in the minocycline-treated group compared to vehicle-treated controls (17.0 ± 2.8 *vs* 31.9 ± 8.6%, $n = 5$, $p < 0.01$, Fig. 5D). Compared to animals receiving vehicle, rats treated with minocycline also achieved significantly better scores in corner turn and forelimb use asymmetry tests after ICH (Fig. 6), indicating better neurological function recovery.

4. Discussion

The major findings of this study are: (1) ICH caused a significant increase in perihematomal brain iron content, iron handling proteins and microglia activation and in aged female rats; (2) the iron overload lasts at least 28 days after ICH; (3) ICH leads to significant short-term brain swelling and long-term brain tissue loss at 28 days in aged female rats; (4) minocycline significantly reduced ICH-induced brain iron overload, attenuated brain injury and improved neurological functional

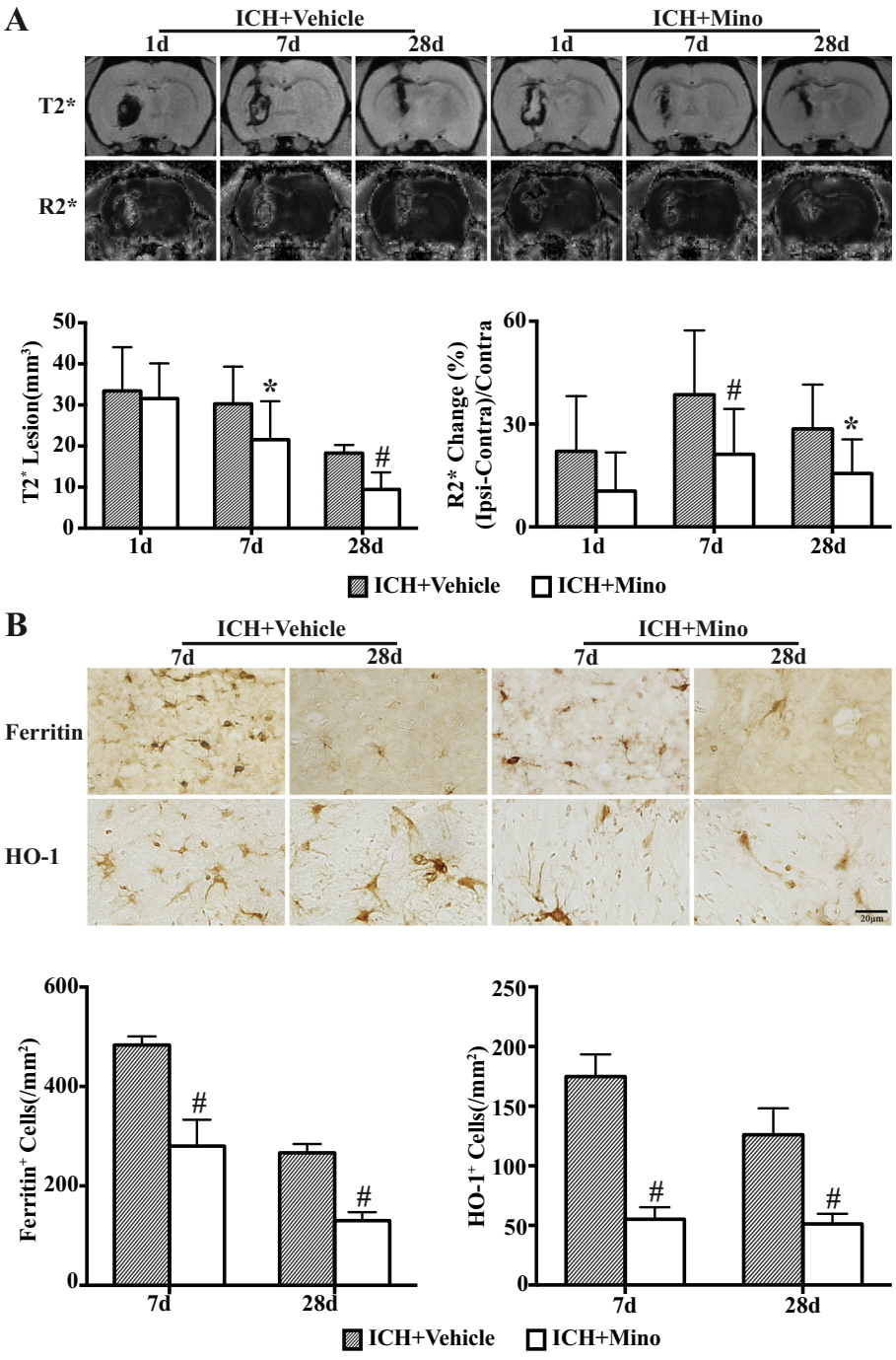

Fig. 4. Effects of minocycline on brain iron and iron handling proteins in aged female rats after ICH. (A) Examples of T2*-weighted and R2* array images from rats treated with vehicle or minocycline (mino) after ICH. The bar graphs show quantification of T2* lesion size and R2* values in the ICH + vehicle and ICH + mino groups at day 1 (n = 16–17), 7 (n = 16–17) and 28 (n = 10–11) after ICH. Values are means ± SD, $^{*}P < 0.05$, $^{\#}P < 0.01$ compared with ICH + vehicle group. (B) Examples of micrographs showing ferritin and HO-1 immunohistochemistry in the ipsilateral basal ganglia at 7 and 28 day after ICH in vehicle and minocycline treated animals. Scale bar = 20 μm. The bar graphs show quantification of the number of ferritin and HO-1 positive cells in the two experimental groups. Values are means ± SD, n = 5 per group; $^{\#}P < 0.01$ compared with ICH + vehicle group.

recovery in aged female rats. Minocycline reduced T2* lesion volume and perihematomal brain iron levels suggesting that minocycline may enhance iron clearance.

The impact of **sex** on neurological disease has been gaining more and more attention in both clinical and preclinical research. Many studies focusing on the difference of treatment, gene expression and underlying mechanisms between male and female after ischemic stroke have revealed that **sex** is a significant factor in determining risk factors and prognosis (Hurn, 2014; Miller et al., 2017). However, research on experimental ICH has mainly used male models. In addition, it is well known that incidence and severity of ICH increases with age (Forti et al., 2016). Our previous study demonstrated that ICH caused more severe brain injury and neurological deficits in aged rats (Gong et al., 2004). Compared to young people (< 65 years), the elderly has 5-fold higher risk of ICH. However, most preclinical research has used young adult animals. The current study, therefore, examined an ICH model in aged female rats to provide an overall picture on the perihematomal iron-related changes within time. Our results indicate that ICH causes reproducible brain swelling, neuronal death and neurological deficits in aged female rats.

Our previous studies showed that minocycline reduces brain injury after ICH in male rats (Cao et al., 2018; Zhao et al., 2011). The current study indicates minocycline can also attenuate ICH-induced brain damage in aged female rats. Sex differences have been found in minocycline treatment in experimental brain ischemia with protection in male mice but not ovariectomized female mice, used to model the post-menopause state (Li and McCullough, 2009). While minocycline therapy is being translated to ICH patients (Fouda et al., 2017), the effectiveness

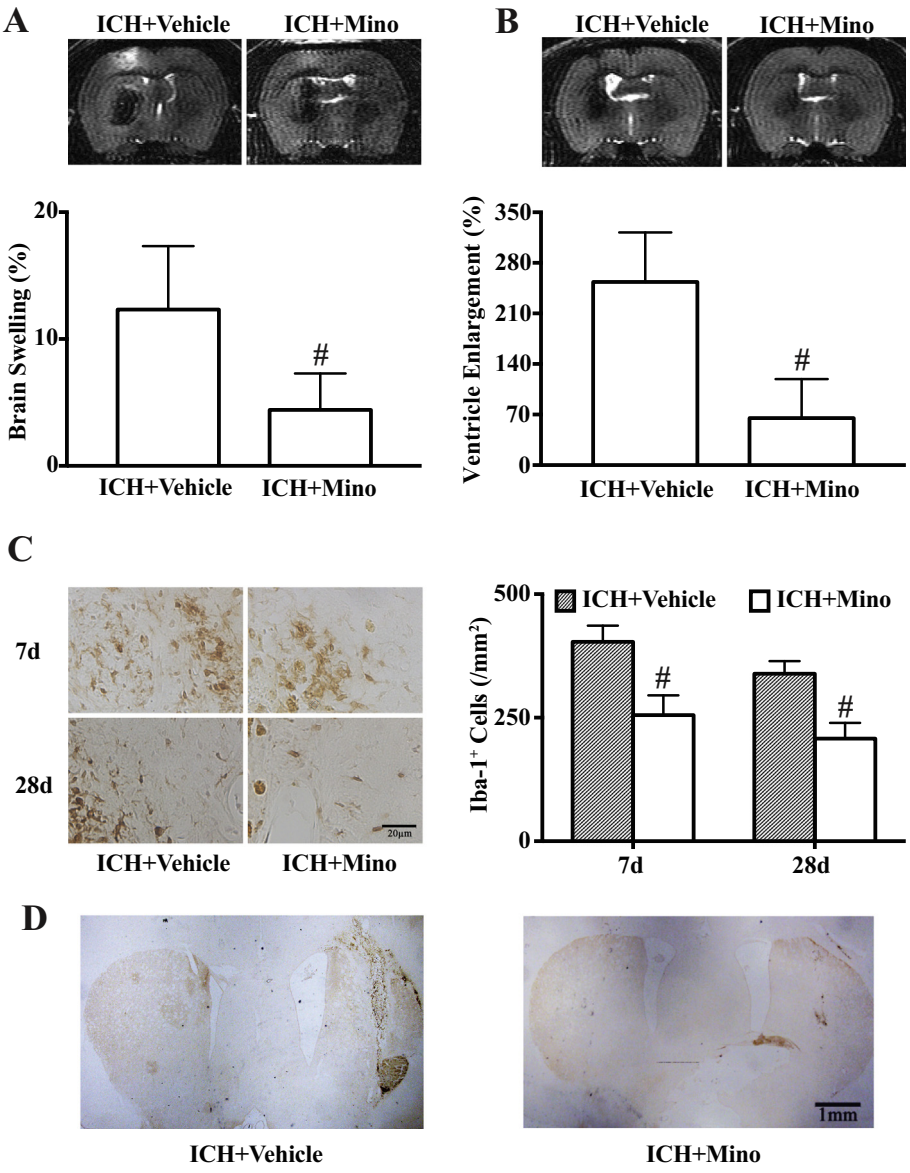

Fig. 5. Effects of minocycline on brain swelling, brain atrophy and microglia activation after ICH. (A) Brain swelling at day 3 ($n = 6$) and (B) brain ventricle enlargement at day 28 ($n = 10$–11) were measured in T2-weighted MRI images (representative scans shown) from minocycline- and vehicle-treated rats. $^{\#}P < 0.01$ compared with ICH + vehicle group. (C) Immunohistochemistry was used to determine Iba-1 positive cells in the ipsilateral basal ganglia at day 7 and 28 after ICH in minocycline and vehicle-treated rats. Representative images are shown (scale bar = 20 μm). The numbers of cells are shown in the bar graph. Values are means ± SD; $n = 6$, $^{\#}P < 0.01$ *vs.* ICH + vehicle group. (D) Representative images of DARPP-32 immunostaining at day 28 after ICH with vehicle or minocycline treatment. Scale bar = 1 mm.

of minocycline on both sexes provides important information for future clinical trials.

ICH accounts for about 10–20% of all strokes (Feigin et al., 2009; Garton et al., 2016). There is substantial preclinical research indicating that hematoma-derived iron induces brain injury after ICH (Haque et al., 2018; Keep et al., 2012; Wilkinson et al., 2018). When red blood cells lyse, hemoglobin may be released into the extracellular space and degradation of that hemoglobin results in iron release. The increased iron contents participate in multiple harmful reactions including free radical production, mitochondria damage and macrophage/microglia activation. As a result, it induces brain edema and cell death after ICH. Although, the underlying mechanisms of iron-induced injury are still not fully understood, preclinical evidence indicates that iron is a key target after ICH in animal models (Garton et al., 2016). Therapeutic treatments with iron chelator such as deferoxamine or minocycline have a promising neuroprotective effect in iron-induced brain injury (Keep et al., 2012). There are current clinical trials for both agents in ICH (Fouda et al., 2017; Selim et al., 2011).

Minocycline is a semisynthetic tetracycline antibiotic, which has strong lipophilic capacity allowing it to cross the blood brain barrier. Minocycline appears to have multiple benefits on brain diseases. However, the underling mechanisms of minocycline-induced neuroprotection are still under investigation while clinical studies have reported varying results. Minocycline is well known as a macrophage/microglia inhibitor *via* various pathways such as poly (ADP-ribose) polymerase-1 (PARP-1) signaling pathway. According to experimental studies, minocycline improved behavioral function, attenuated neural apoptosis, suppressed free radical production and inhibited matrix metalloproteinases both in ischemic and hemorrhagic stroke (Kohler et al., 2013). In the current study, minocycline did reduce the number of Iba-1 positive microglia/macrophages after ICH. However, minocycline has also been found to have potential iron-chelating characteristics both *in vivo* and *in vitro* (Cao et al., 2018; Chen-Roetling et al., 2009). In our previous studies, we found that minocycline reduces iron overload and attenuates neurological deficits after ICH as well as iron-induced brain injury in young male Sprague-Dawley rats (Zhao et al., 2011) and in aged male F344 rats (Cao et al., 2018). One potential reason why minocycline demonstrated protection in the current study of ICH in aged female rats but was not protective in a study examining ischemic injury in ovariectomized female mice (Li and McCullough, 2009) is the relative role of iron in the two forms of stroke. While both ICH and cerebral ischemia induce neuroinflammation, ICH has the potential to cause greater iron overload.

Minocycline has some adverse effects. For example, while a large

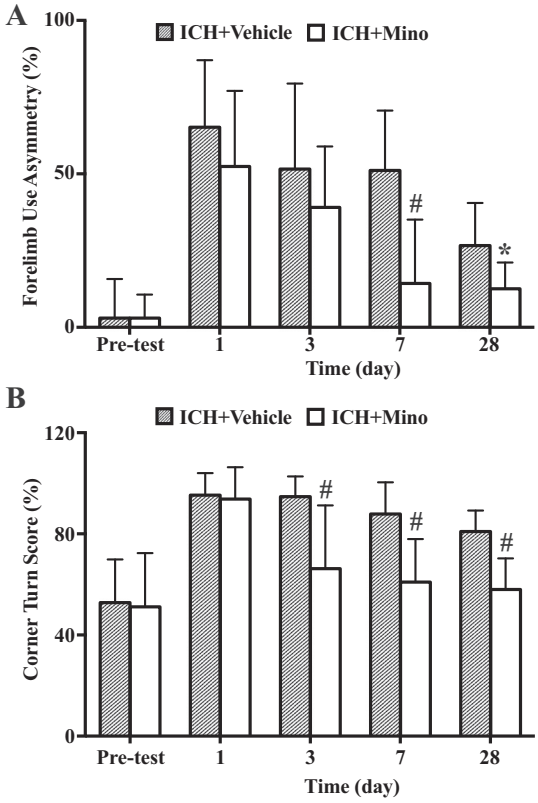

Fig. 6. Effects of minocycline on functional recovery in aged female rats after ICH. Forelimb use asymmetry (A) and corner turn (B) tests were performed pre-ICH (n = 16–17) and at day 1 (n = 16–17), 3 (n = 16–17), 7 (n = 16–17) and 28 (n = 10–11) after ICH in minocycline and vehicle treated rats. $^{*}P < 0.05$ and $^{\#}P < 0.01$ compared with ICH + vehicle group.

dose (45 mg/kg) is safe for young animals, the dose resulted in high mortality in aged ICH rats. Therefore, we used 20 mg/kg for the initial dose. Minocycline also has immunomodulatory effects and can induce lupus erythematosus (Schlienger et al., 2000). To translate minocycline to a potential clinical trial for ICH patients, an optimal dose, an optimal duration and a therapeutic time window should be determined in aged animals and/or large gyrencephalic species. Potential adverse effects of minocycline should be examined in translational studies because minocycline can worsen outcomes in amyotrophic lateral sclerosis patients (Gordon et al., 2007). To reduce systemic minocycline-induced side effects, it would be interesting to know whether intranasal or intrahematomal delivery of minocycline is effective.

Ferritin is both a marker of iron overload and a protector against such overload. As a naturally occurring iron chelator and a major storage protein for iron in brain, ferritin is essential in maintaining iron homeostasis and increases in respond to iron overload. A logistic regression analysis of clinical studies showed that high serum ferritin levels on day 1 and day 7 independently correlate with poorer clinical outcomes at 3 months after ICH (Garton et al., 2017). In contrast, a study on cortical cell cultures has shown that the neuroprotective effect of minocycline on iron-induced neuron injury has a relationship with increased ferritin levels (Chen-Roetling et al., 2009). In the current study, minocycline reduced perihematomal ferritin levels in aged female rats at days 7 and 28. This suggests that minocycline suppresses free iron levels, thereby reducing ferritin expression both at an early and late stage after ICH. This suggestion is supported by the data on perihematomal iron levels using R2* mapping.

Minocycline may also protect the brain tissues from ICH-induced oxidative stress, indicated by the downregulation of HO-1 expression in perihematomal areas. In the current study, HO-1 positive cells were microglia-like cells. Our previous study also showed that macrophages are HO-1 positive (Cao et al., 2016). HO-1 degrades heme releasing iron. Increased HO-1 level after ischemic-reperfusion brain injury may contribute to increased infarct volume (Jiang et al., 2017). However, HO-1 upregulation may have neuroprotective effects after brain trauma while inhibition of heme oxygenase had beneficial effects in animal models of ICH (Keep et al., 2012). Therefore, further research on the effects and mechanisms of minocycline on endogenous response including the effects of minocycline on microglia/macrophage polarization are needed to fully understand its role in ICH-induced brain injury.

ICH-induced brain iron overload is different in males and females. For example, brain iron contents peaked at two weeks after ICH in aged male rats (Cao et al., 2018). However, ICH caused less severe brain iron overload, which peaked at 3 days following ICH in females. The sex difference of ICH-induced brain iron overload needs to be examined further.

In conclusion, we found that perihematomal iron content, iron handling proteins and microglia activation all increased in an aged female rat ICH model. Systemic administration of minocycline reduced ICH-induced brain iron overload, brain injury and neurological deficits in that model.

Conflict of interest

None.

Acknowledgements

This study was supported by grants NS-091545, NS-090925, NS-096917, and NS-106746 from the National Institutes of Health (NIH).

References

Cao, S., et al., 2016. Hematoma changes during clot resolution after experimental intracerebral hemorrhage. Stroke 47, 1626–1631.
Cao, S., et al., 2018. Minocycline effects on intracerebral hemorrhage-induced iron overload in aged rats: brain iron quantification with magnetic resonance imaging. Stroke 49, 995–1002.
Chen, M., Regan, R.F., 2007. Time course of increased heme oxygenase activity and expression after experimental intracerebral hemorrhage: correlation with oxidative injury. J. Neurochem. 103, 2015–2021.
Chen-Roetling, J., et al., 2009. Minocycline attenuates iron neurotoxicity in cortical cell cultures. Biochem. Biophys. Res. Commun. 386, 322–326.
Dang, G., et al., 2017. Early erythrolysis in the hematoma after experimental intracerebral hemorrhage. Transl Stroke Res 8, 174–182.
Feigin, V.L., et al., 2009. Worldwide stroke incidence and early case fatality reported in 56 population-based studies: a systematic review. Lancet Neurol. 8, 355–369.
Fisher, M., et al., 2009. Update of the stroke therapy academic industry roundtable preclinical recommendations. Stroke 40, 2244–2250.
Forti, P., et al., 2016. The effect of age on characteristics and mortality of intracerebral hemorrhage in the oldest-old. Cerebrovasc. Dis. 42, 485–492.
Fouda, A.Y., et al., 2017. Minocycline in acute cerebral hemorrhage: an early phase randomized trial. Stroke 48, 2885–2887.
Garton, T., et al., 2016. Brain iron overload following intracranial haemorrhage. Stroke Vasc. Neurol. 1, 172–184.
Garton, A.L.A., et al., 2017. Biomarkers of functional outcome in intracerebral hemorrhage: interplay between clinical metrics, CD163, and ferritin. J. Stroke Cerebrovasc. Dis. 26, 1712–1720.
Gong, Y., et al., 2004. Intracerebral hemorrhage: effects of aging on brain edema and neurological deficits. Stroke 35, 2571–2575.
Gordon, P.H., et al., 2007. Efficacy of minocycline in patients with amyotrophic lateral sclerosis: a phase III randomised trial. Lancet Neurol. 6, 1045–1053.
Haque, M.E., et al., 2018. Serial quantitative neuroimaging of iron in the intracerebral hemorrhage pig model. J. Cereb. Blood Flow Metab. 38, 375–381.
Hua, Y., et al., 2002. Behavioral tests after intracerebral hemorrhage in the rat. Stroke 33, 2478–2484.
Hurn, P.D., 2014. 2014 Thomas Willis award lecture: sex, stroke, and innovation. Stroke 45, 3725–3729.
Jiang, L.J., et al., 2017. Roles of the Nrf2/HO-1 pathway in the anti-oxidative stress response to ischemia-reperfusion brain injury in rats. Eur. Rev. Med. Pharmacol. Sci. 21, 1532–1540.
Jin, H., et al., 2013. DARPP-32 to quantify intracerebral hemorrhage-induced neuronal death in basal ganglia. Transl Stroke Res 4, 130–134.
Keep, R.F., et al., 2012. Intracerebral haemorrhage: mechanisms of injury and therapeutic targets. Lancet Neurol. 11, 720–731.

Kohler, E., et al., 2013. Intravenous minocycline in acute stroke: a randomized, controlled pilot study and meta-analysis. Stroke 44, 2493–2499.
Li, J., McCullough, L.D., 2009. Sex differences in minocycline-induced neuroprotection after experimental stroke. J. Cereb. Blood Flow Metab. 29, 670–674.
Mao, S., et al., 2016. Role of lipocalin-2 in thrombin-induced brain injury. Stroke 47, 1078–1084.
Miller, L.R., et al., 2017. Considering sex as a biological variable in preclinical research. FASEB J. 31, 29–34.
Murata, Y., et al., 2008. Extension of the thrombolytic time window with minocycline in experimental stroke. Stroke 39, 3372–3377.
Nakamura, T., et al., 2004. Deferoxamine-induced attenuation of brain edema and neurological deficits in a rat model of intracerebral hemorrhage. J. Neurosurg. 100, 672–678.
Ni, W., et al., 2015. Role of lipocalin-2 in brain injury after intracerebral hemorrhage. J. Cereb. Blood Flow Metab. 35, 1454–1461.
Schlienger, R.G., et al., 2000. Minocycline-induced lupus. A systematic review. Dermatology 200, 223–231.
Selim, M., et al., 2011. Safety and tolerability of deferoxamine mesylate in patients with acute intracerebral hemorrhage. Stroke 42, 3067–3074.
Truman-Rosentsvit, M., et al., 2018. Ferritin is secreted via 2 distinct nonclassical vesicular pathways. Blood 131, 342–352.
Wang, J., Dore, S., 2007. Inflammation after intracerebral hemorrhage. J. Cereb. Blood Flow Metab. 27, 894–908.
Wilkinson, D.A., et al., 2018. Hematoma clearance as a therapeutic target in intracerebral hemorrhage: from macro to micro. J. Cereb. Blood Flow Metab. 38, 741–745.
Xi, G., et al., 2006. Mechanisms of brain injury after intracerebral haemorrhage. Lancet Neurol. 5, 53–63.
Zhao, F., et al., 2011. Minocycline-induced attenuation of iron overload and brain injury after experimental intracerebral hemorrhage. Stroke 42, 3587–3593.